Eur. Phys. J. D **37**, 319–325 (2006)
DOI: 10.1140/epjd/e2005-00316-1

THE EUROPEAN PHYSICAL JOURNAL D

Desorption of Rb and Cs from PDMS induced by non resonant light scattering

C. Marinelli[1], A. Burchianti[1], A. Bogi[1], F. Della Valle[2], G. Bevilacqua[1,a], E. Mariotti[1], S. Veronesi[1], and L. Moi[1]

[1] Università di Siena, Dipartimento di Fisica, Via Roma 56, 53100 Siena, Italy
[2] Università di Trieste, Dipartimento di Fisica, via A. Valerio 2, 34127 Trieste, Italy

Received 1st September 2005
Published online 22 November 2005 –

Abstract. Simultaneous light-induced desorption of rubidium and cesium atoms has been observed in polydimethylsiloxane (PDMS) coated Pyrex cells at room temperature and at low light intensity. The two alkali atoms show the same dynamics and the same dependence on the desorbing light frequency. No competition in the free sites occupancy exists. An interpretation of the experimental results in terms of non-resonant light scattering from the PDMS coating is discussed.

PACS. 68.43.Tj Photon stimulated desorption – 34.50.Dy Interactions of atoms and molecules with surfaces; photon and electron emission; neutralization of ions

1 Introduction

The term "Light-Induced Atomic Desorption" (LIAD) has been spreadingly used to indicate an extended class of physical effects that are due to the simultaneous interaction of light, atomic vapours and atoms adsorbed on rough surfaces or substrates. In fact, LIAD can be observed either with weak illumination conditions, when the local temperature is constant [1–7], or in the presence of quite intense light pulses followed by strong heating of the adsorbant [8,9]. On the other hand, LIAD has been studied in metallic surfaces, Pyrex, sapphire or quartz, porous glasses [10], organic films, producing desorption of different atomic and molecular species. At low or moderate light intensities, delivered even by non coherent and non resonant sources, huge amounts of Na, K, Rb and Cs atoms have been obtained from desorption in cells coated with polydimethylsiloxane (PDMS) [1–6], octamethylcyclotetrasiloxane (OCT) [5] and paraffin [7,11]. Surprisingly, these are the same coatings used in optical pumping experiments because of their property of preserving spin orientation in the atom-wall collisions, due to very low adsorption energy [12,13]. LIAD has been also proved useful to prepare a light-controlled Rb atomic source at room temperature [14], and to load at a very fast rate and with a very high efficiency a Magneto-Optical Trap (MOT) [9,15]. More recently, LIAD from a Pyrex helix has been used to load a Bose-Einstein Condensate (BEC) in a portable atom-chip system [16].

Detailed experimental analysis of the LIAD effect from organic films has been made in the last few years measuring either the vapour density changes in sealed cells or the atomic velocity distribution in vacuum chambers with the Time of Flight (TOF) technique [17]. In particular, measurements have been done as a function of film temperature, desorbing light intensity and frequency, illumination time [4,5]. Experiments clearly show that atomic diffusion inside the coating, both with and without cell illumination, plays a major role in the effect. Therefore, in this context, LIAD is not a simple surface effect.

Even if a lot of phenomenological information has been accumulated about LIAD, a detailed description of the interaction mechanisms between light, atom and organic film is still lacking. A convincing theoretical model should take into account the fact that the atoms inside the film experience interactions with different partners. These interactions correspond to very different energies that range from values typical of weakly bound states (physisorption) to values typical of strongly bound states (chemisorption). In a qualitative picture, one can say that chemisorbed atoms cannot move around, while physisorbed atoms are able to drift, even at room temperature and in absence of light, from one site to the next one. This picture explains for example why no LIAD effect is observed when the cell is new: atoms diffuse from one shallow potential site to the next one, till they are captured in deep potential wells; only when these sites are filled up the diffusing atoms are free to move around, slowly in the dark, faster in the presence of light. In order to further test the LIAD mechanism and to explore the possibility to set-up light-controlled atomic dispensers delivering one or more species, we have prepared PDMS coated and sealed cells where both rubidium and cesium have been distilled. This

[a] e-mail: bevilacqua@unisi.it

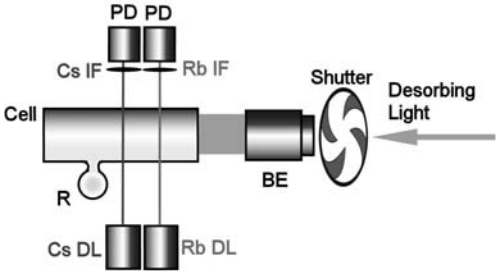

Fig. 1. Experimental set-up: R = Rb + Cs reservoir; BE = beam expander; PD = photodiodes; IF = interference filter at 795 nm (Rb) and 852 nm (Cs); DL = diode laser systems.

approach allows us to directly compare the behaviour of the two alkali atoms without suffering from the possible differences in thickness, purity, homogeneity, defects existing between the cells. Preliminary results have been already reported in reference [18]. A similar approach has also been adopted by Alexandrov et al. [7] with paraffin coated cells. The experimental results, quite similar to those reported in reference [7], can be summarized as follows: first, no competition exists between Rb and Cs in occupying the free sites inside the coating; second, no significant differences exist between the two alkalis in the dynamics and in the frequency dependence of LIAD. These facts lead us to propose an interpretation that does not depend on the energy levels of the two atomic species, but on the quite general phenomenon of non resonant light scattering.

2 Experimental apparatus and results

The experimental apparatus is sketched in Figure 1. Measurements have been performed with three cells filled with different Rb and Cs amalgams that give vapour densities in a ratio 7:1, 3:1 and 1:1 respectively. As all the cells show the same behaviour, in the following we will make specific reference to the cell with 1:1 vapour density ratio, that makes the absorption signals directly comparable. This cell is a Pyrex glass cylinder (total length 62 mm; external diameter 20 mm) coated with a PDMS film. Cell preparation followed the standard procedure: the cell is carefully cleaned, baked and rinsed with an ether solution of a few percent PDMS; when ether has evaporated the cell is placed for a few hours in an oven heated up to about 200 °C and then connected to a vacuum pump for a day. An uncoated Rb and Cs reservoir is then welded to the cell that is then left connected to the vacuum system for several days. As we said before, the Rb and Cs vapour densities in the cell at room temperature are the same within 10%; it is however important to remark that in coated cells the vapour density is normally lower than in uncoated ones at thermal equilibrium. This difference usually ranges in the order of a few per cent, but it can be much larger. Small deviations are attributed to continuous adsorption of atoms into the organic coatings, large ones to possible contamination of the metal reservoir by the coating itself [7,12,13,19,20]. In our cell the measured Rb density was about 13% of the equilibrium vapour density [21] and Cs density about 2.4%, within 10% uncertainty [22].

Two diode lasers tuned to the Rb D_1 line and to the Cs D_2 line respectively, generate the probe beams. Their intensities have been reduced by means of neutral filters in order to make negligible hyperfine pumping and avoid saturation of the transitions. The transmission signals are detected by two photodiodes and sent to the data acquisition system that allows us to collect data simultaneously with the same accuracy for both alkali atoms during several hours. The desorption-adsorption processes are monitored through the changes in the vapour densities n_{Rb} and n_{Cs} of the two alkali atoms when desorbing light is on or off. The diode laser frequencies are swept at a few hertz rate and the absorption spectra continuously acquired. The density changes are evaluated by fitting the atomic line profiles. In order to make a thorough analysis as a function of desorbing light frequency, different light sources have been used: an Ar^+ laser, several diode lasers, a dye laser, a high pressure Hg lamp. In all the measurements the cell has been illuminated in the same way with all the light sources. At the beginning the cell had to be exposed for few days to alkali atoms in order to observe LIAD effect with stable features for both Rb and Cs.

2.1 LIAD dynamics

Vapour density changes induced by desorbing light are conveniently described by the quantities:

$$\delta_{\mathrm{Rb,Cs}}(t) = \frac{n_{\mathrm{Rb,Cs}}(t) - n_{\mathrm{Rb,Cs}}(0)}{n_{\mathrm{Rb,Cs}}(0)} \qquad (1)$$

where $n_{\mathrm{Rb}}(0)$ and $n_{\mathrm{Cs}}(0)$ represent the Rb and Cs vapour densities at room temperature when the cell is at equilibrium in the dark. Usually the cell is illuminated for a given time interval, then the desorbing light is switched off. Typical results are reported in Figure 2 for three different frequencies and intensities of the desorbing light. The time dependence shows several features that can be reproduced by our theoretical model presented in references [4,5]. The model takes into consideration atomic diffusion inside the PDMS and an increased mobility in the presence of light. The Rb and Cs normalized absorption signals increase during the illumination time up to a maximum and then decrease, returning to the equilibrium values once the light is switched off. The important point to be stressed here is that the relative vapour density changes are always the same for both alkalis even when they are as large as one order of magnitude. The graphs of $\delta_{\mathrm{Rb}}(t)$ and $\delta_{\mathrm{Cs}}(t)$ have so much the same behaviour that it is not easy to distinguish one from the other. For this reason the quantity $\Delta(t) = \delta_{\mathrm{Rb}}(t) - \delta_{\mathrm{Cs}}(t)$ is shown at the bottom of each plot. The difference $\Delta(t)$ remains below a few per cent even after many illumination-dark cycles and a total exposition time of a few hours, as shown in Figure 3. It is interesting to remark that $\delta_{\mathrm{Rb}}(t)$ and $\delta_{\mathrm{Cs}}(t)$ reach lower

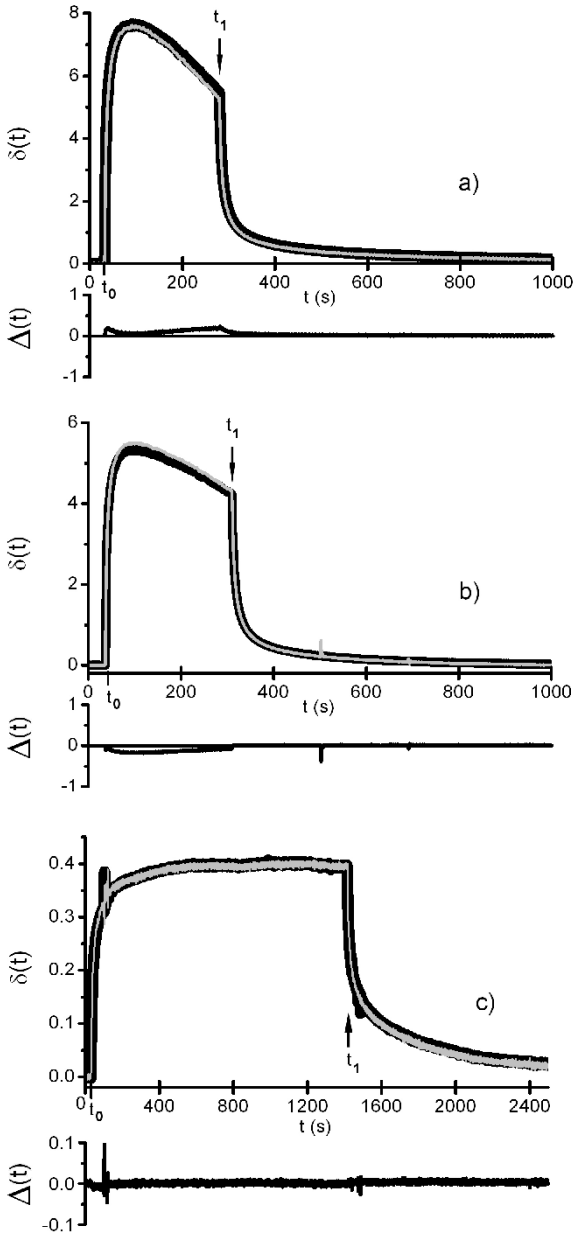

Fig. 2. Relative vapour density changes $\delta(t)$ of Rb (black curves) and Cs (grey curves) upon different illumination conditions: (a) $\lambda = 476$ nm, $I_L = 80$ mW/cm^2; (b) $\lambda = 514$ nm, $I_L = 80$ mW/cm^2; (c) $\lambda = 810$ nm, $I_L = 30$ mW/cm^2. Desorbing light is switched on at time t_0 and off at time t_1. The curves at the bottom of each plot give the difference between the two $\delta(t)$.

and lower maximum levels from one illumination period to the next one because the coating is progressively emptied. This is due both to desorption and to the fact that atomic diffusion inside the coating is faster in the presence of light than in the dark [5]. We remind that the time scale to restore equilibrium is such that we are able to perform only one measurement per day.

The fact that $\Delta(t)$ is, in the limit of our accuracy, constant and close to zero supports the following points: (i) no competition between the two alkalis takes place inside the coating; (ii) the atomic diffusion in the coating is the same for both alkalis, both in the dark and in the presence of light; (iii) the effect does not depend on specific properties (for example energy levels and polarizability) of the two atoms.

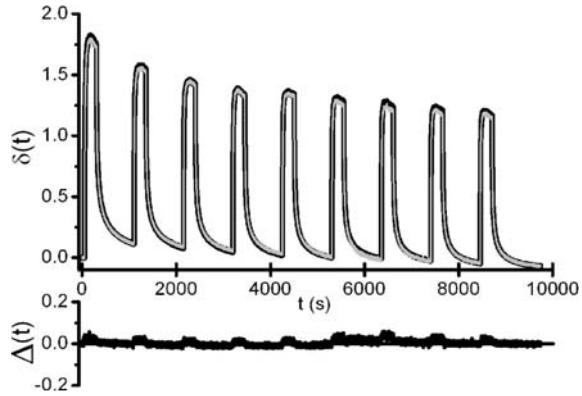

Fig. 3. Relative vapour density changes $\delta(t)$ of Rb and Cs upon multiple illumination conditions provided by an argon ion laser $\lambda = 514$ nm, $I_L = 7$ mW/cm^2. Black curve and grey curve give $\delta_{\mathrm{Rb}}(t)$ and $\delta_{\mathrm{Cs}}(t)$ respectively. The curve at the bottom of the plot gives the difference between the two $\delta(t)$.

2.2 LIAD as a function of desorbing light intensity

Following the same approach developed in previous works [4,5], we introduce the parameters

$$\delta^{max}_{\mathrm{Rb,Cs}} = \frac{n^{max}_{\mathrm{Rb,Cs}} - n_{\mathrm{Rb,Cs}}(0)}{n_{\mathrm{Rb,Cs}}(0)} \tag{2}$$

and

$$R_{\mathrm{Rb,Cs}} = \frac{1}{n_{\mathrm{Rb,Cs}}(0)} \left(\frac{dn_{\mathrm{Rb,Cs}}}{dt} \right)_{t=t_0} \tag{3}$$

where $\delta^{max}_{\mathrm{Rb,Cs}}$ give the maximum relative increases of Rb and Cs vapour densities and $R_{\mathrm{Rb,Cs}}$ are the relative increasing rates of the two vapour densities immediately after the desorbing light switching on at $t = t_0$. In agreement with our model and with previous experimental results with Rb and Cs cells, δ^{max} should show a square root dependence on desorbing light intensity, whereas R should be linear with intensity [4,5]. In Figure 4, plots of $(\delta^{max}_{\mathrm{Rb,Cs}})^2$ and $R_{\mathrm{Rb,Cs}}$ as functions of the desorbing light intensity at selected wavelengths are shown. The experimental results are in a good agreement with the model and, at the same time, show that the two atomic species have the same behaviour, within the error bars, in all the experimental conditions checked.

The linear best fits of $R_{\mathrm{Rb,Cs}}$ plotted as functions of the desorbing light intensity I_L give the linearity coefficients of the relations

$$R_{\mathrm{Rb,Cs}}(\lambda) = k_{\mathrm{Rb,Cs}}(\lambda) I_L \tag{4}$$

The values of $k_{\mathrm{Rb,Cs}}$, in units of cm^2/J, have been derived for each desorbing light wavelength and are reported in

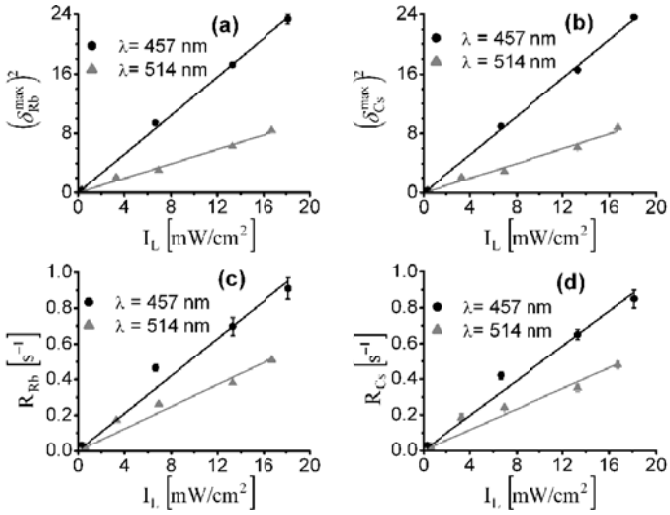

Fig. 4. (a) and (b): $(\delta^{max}_{\mathrm{Rb,Cs}})^2$ as a function of desorbing light intensity for two different desorbing light wavelengths; (c) and (d): $R_{\mathrm{Rb,Cs}}$ as a function of desorbing light intensity for two different desorbing light wavelengths.

Table 1. Desorbing rate k (in cm^2/J), number of desorbed atoms per unit energy η (in atom/J $\times 10^{10}$) and number of desorbed atoms per photon γ (in atom/ph $\times 10^{-8}$) for various desorbing light wavelengths.

λ_{des} (nm)	k_{Rb} k_{Cs}	η_{Rb} η_{Cs}	γ_{Rb} γ_{Cs}
457	52±3	11±1	4.7±0.4
	49±3	11±1	4.7±0.4
476	49±3	10±0.8	4.2±0.4
	48±2	11±1	4.6±0.4
488	36±2	7.4±0.6	3.0±0.3
	35±2	8.0±0.7	3.3±0.3
514	31±2	6.3±0.5	2.5±0.2
	29±2	6.7±0.6	2.6±0.2
590	13±1	2.7±0.2	0.92±0.08
	13±1	2.9±0.2	1.0±0.1
685	3.9±0.2	0.80±0.06	0.23±0.02
	3.7±0.2	0.85±0.07	0.25±0.02
787	1.6±0.2	0.20±0.02	0.050±0.004
	1.5±0.1	0.35±0.03	0.09±0.01
810	1.3±0.2	0.19±0.02	0.048±0.004
	1.1±0.1	0.25±0.02	0.060±0.005

Table 1. The measurements of $k_{\mathrm{Rb,Cs}}$ allow us to evaluate the effective numbers $\eta_{\mathrm{Rb,Cs}}$ of atoms desorbed per unit energy of incident light, given by

$$\eta_{\mathrm{Rb,Cs}}(\lambda) = k_{\mathrm{Rb,Cs}}(\lambda) n_{\mathrm{Rb,Cs}}(0) L \qquad (5)$$

where L is a characteristic length defined as the ratio of the cell volume and the illuminated surface. The values of $\eta_{\mathrm{Rb,Cs}}$ are also reported in Table 1.

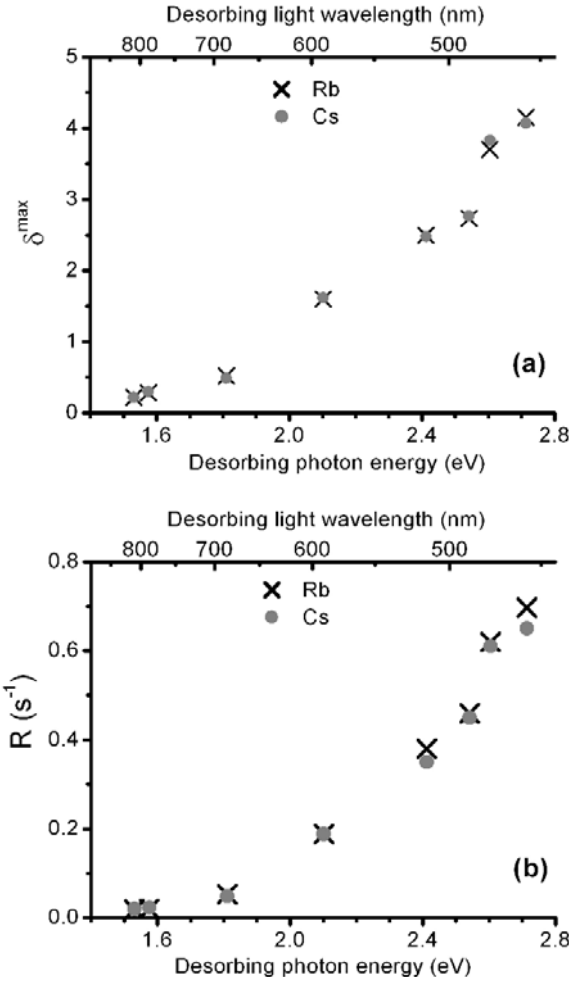

Fig. 5. (a) Maximum relative changes of vapour density $\delta^{max}_{\mathrm{Rb,Cs}}$ and (b) initial relative increasing rate $R_{\mathrm{Rb,Cs}}$ as functions of desorbing photon energy. The desorbing light intensity is $I_L = 13$ mW/cm^2.

2.3 LIAD as a function of light frequency

We have observed LIAD effect induced by light with wavelength in the 300–1064 nm range and a systematic study has been done in the 457–810 nm range. Plots of δ^{max} and R versus desorbing photon energy are given in Figure 5 for constant desorbing light intensity and illuminated area. The effect increases with the desorption photon energy for both atoms and no resonances are observed. The calculated $\eta_{\mathrm{Rb,Cs}}$ values are essentially the same for the two atomic species and show a desorption efficiency decreasing by about a factor 50 when the desorbing light wavelength changes from 457 nm to 810 nm. The desorption efficiencies $\gamma_{\mathrm{Rb,Cs}}$, defined as the number of desorbed atoms per photon, are also reported in Table 1 and plotted in Figure 6 versus desorbing photon energy (the line curves presented in the figure will be discussed in the next section). Measured efficiencies fall in the $10^{-8} \div 10^{-10}$ range. We note that γ is defined as a general parameter that can be used to describe any LIAD processes, independently of the experimental details. It is not equivalent and therefore

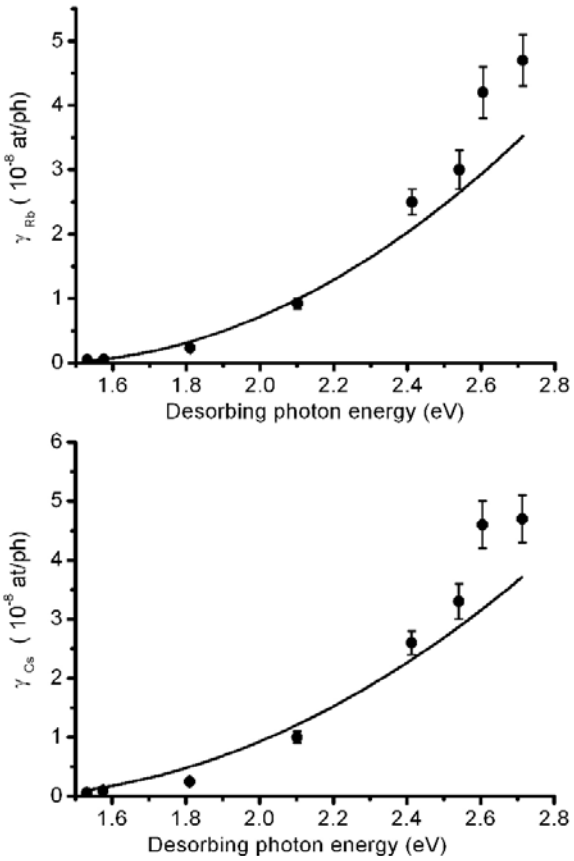

Fig. 6. Experimental desorption efficiencies γ from the data of Table 1, as functions of desorption photon energy (see Sect. 2.3). Continuous line is the best fit of the data with the function in equation (6) (see Sect. 3).

cannot be compared to a previous definition of efficiency as the ratio of the total number of atoms, accumulated in the vapour phase, to the overall estimated number of photons hitting the cell during the illumination time [14]. This definition is strongly dependent on the gas dynamics of the cell that, in case cited, was also filled with a few Torr of buffer gas.

3 Discussion

In Figure 7 the absorbance of PDMS, obtained by using a spectrophotometer, is reported for a sample thickness of 1 cm. Pure PDMS shows huge absorption in the IR and UV regions, but it is transparent in the visible. The measured absorbance in the 400–800 nm region is about 0.03, corresponding to a change in the light intensity of about 7%. As we estimate that film thickness in our cell is of the order of a few microns, the total scattering processes in the substrate involve about one photon in 10^5. LIAD effect can thus be thought to contribute at most a very small correction to the whole attenuation, but it has a clearly different and typical frequency dependence. All these facts rule out the possibility that LIAD may depend on a resonant process. The experimental evidence

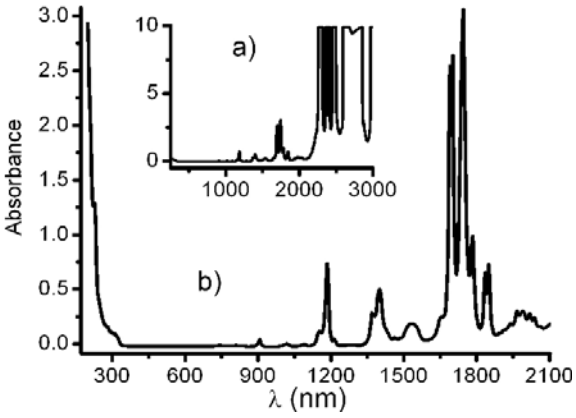

Fig. 7. Absorbance of a pure PDMS sample of 1 cm thickness measured with a commercial spectrophotometer.

that LIAD in the PDMS system does not show an appreciable dependence on the atomic species and that it is not related to direct light absorption by the coating itself are key points to infer an explanation of the effect.

An interpretation of the effect was proposed by Gozzini et al. [2,23] for Na adsorbed on PDMS. According to their model, sodium atoms are solvated in the siloxane compound and the Na^+PDMS^- complex is formed. The desorbing light should induce a reverse mechanism that brings back atoms in the vapour phase, in analogy with the photoelectric effect. This approach to LIAD as a photoatomic effect supports the experimental results of Gozzini et al. about the presence of a threshold in the desorbing light frequency, but confines the effect to the surface, neglecting the atomic diffusion inside the coating. Moreover it imposes resonance conditions to the light frequency that should strongly depend on the specific alkali atom. This picture has been recently adopted also by Rubahn and coworkers [24] to explain the outcome of their desorption experiments. In this case pulsed lasers are used to desorb Na atoms showing quite high kinetic energies. A resonant process is supposed to bring atoms from a deep potential well to a repulsive state while the excess energy is transformed into kinetic energy. In that work the two 1064 nm and 532 nm wavelengths from a Nd–Yag laser are used, in order to excite two different electronic levels of the complex. This imposes two resonance conditions that make stronger the correlation between the effect and the selected alkali atom. No analysis at intermediate wavelengths has been done. In our case and in the work on paraffin [7] no correlation with the energy levels of the free atoms is seen. Moreover, the model based on electronic resonance implies the presence of a frequency threshold in the desorbing light that should be obtained by fitting the data with the function [23]

$$\gamma = \alpha \left(h\nu - h\nu_{th}\right)^2 \tag{6}$$

where ν_{th} is the threshold frequency. We have fitted our data using the function of equation (6). The curves, plotted in Figure 6, show that the function does not properly describe the high energy behavior of the experimental

data. Moreover we get, for both Rb and Cs, a threshold at $h\nu_{th} = 1.4 \pm 0.2$ eV, corresponding to a wavelength $\lambda_{th} \approx 900$ nm. This result is contradicted by our observation of LIAD with longer wavelengths and by the data of Brewer et al. [17], who have evidence of LIAD effect with excitation at 1064 nm. Therefore a different explanation of the effect has to be found.

Let us consider the PDMS substrate as composed of a non-regular collection of polymer chains in an amorphous ("liquid") state of aggregation (see for example Ref. [25]). The alkali atoms can be physisorbed in potential wells of different sizes and depths along the chains or in the interstitial regions. We believe that the alkali density inside the coating is low enough to neglect adatoms interactions. Let us suppose that these wells have only few vibrational bound states. In the presence of chain vibrations these bound levels become not stationary and the alkali atoms can be scattered by phonons either to higher vibrational levels or to the nearest-neighbour sites. This of course gives a mechanism to the diffusion inside the coating and to adsorption-desorption of the atoms at room temperature and in the dark (see Ref. [26] and references quoted therein). When light illuminates the coating apparently no resonant processes take place. So we are left only with non resonant inelastic light scattering (Raman and Brillouin type). We expect that elastic or Rayleigh scattering should play a minor role because it can only act on the wave vector of the phonons, without any energy exchange between light and molecules. In the inelastic scattering, on the contrary, energy exchange is allowed and more phonons can be excited. For example, the standard microscopic description of Raman scattering in semiconductors involves an electronic transition stimulated by the incident photon, then an inelastic scattering process between the excited electron and some phonons and eventually the electron jumps in the valence band re-emitting a slightly less-energetic photon. Notice that the energy must be conserved only in the overall process. We postulate a similar mechanism in the interaction between light and PDMS substrate in order to explain the energy transfer between light and the PDMS and then the final desorption of alkali atoms mediated by phonons. The scattering process can be described without involving the electrons but rather the atomic motion of the chain elements [27–29]. Generally speaking this "ionic" Raman effect is usually very small and is dominated by the electronic one, but in our case it should play some role. First, because in the IR region it is impossible to excite non-virtual electronic transitions. Second, because the scattering cross-section, in the presence of localized vibrational modes due for instance to impurities or imperfection, can become relevant [27–29].

In a previous paper [5] we have measured the diffusion changes induced by light and we obtained a relative increase of the order of 100 for the diffusion coefficient and of the order of 1000 for the desorption rate. According to reference [30], the average dwelling time of an atom in one site is given by

$$\tau_s = \tau_0 \, \exp\left(\frac{E_0}{kT}\right) \tag{7}$$

with τ_0 of the order of 10^{-12} s. From this we get for the ratio of the dwelling times in the presence ($\tau_{s,L}$) and in the absence ($\tau_{s,D}$) of light

$$\frac{\tau_{s,D}}{\tau_{s,L}} = \exp\left(\frac{\Delta E}{kT}\right) \approx 10^2 \div 10^3 \tag{8}$$

corresponding to a binding energy change ΔE equal to few kT. Such small energy change supports the picture that light excites phonons inside the coatings with a transfer of energy to the most loosely bound atoms that are then desorbed. As a last remark, our estimation of the effect (see Tab. 1) gives an efficiency in terms of atoms desorbed per photon in the range $10^{-8} \div 10^{-10}$, that is compatible with the probability of non resonant light scattering. A quantitative model taking into account the atom-phonon interaction is required for a deeper understanding of the desorption process. More detailed studies on the subject are ongoing.

We would like to thank S. Sanguinetti for the spectrophotometer measurements, M. Badalassi for cell manufacturing and all the people from the mechanical and electronic workshops of the Physics Department. This work was partially financed by European Communityâs Human Potential Programme under contract HPRN-CT-2002-00304, "FASTnet".

References

1. M. Meucci, E. Mariotti, P. Bicchi, C. Marinelli, L. Moi, Europhys. Lett. **25**, 639 (1994)
2. A. Gozzini, F. Mango, J.H. Xu, G. Alzetta, F. Maccarrone, R.A. Bernheim, Nuovo Cim. D **15**, 709 (1993)
3. E. Mariotti, M. Meucci, C. Marinelli, P. Bicchi, L. Moi, *XIIth International Conference on Laser Spectroscopy* (World Scientific, New York, 1996), p. 390
4. S.N. Atutov, V. Biancalana, P. Bicchi, C. Marinelli, E. Mariotti, M. Meucci, A. Nagel, K.A. Nasyrov, S. Rachini, L. Moi, Phys. Rev. A **60**, 4693 (1999)
5. C. Marinelli, K.A. Nasyrov, S. Bocci, B. Pieragnoli, A. Burchianti, V. Biancalana, E. Mariotti, S.N. Atutov, L. Moi, Eur. Phys. J. D **13**, 231 (2001)
6. S. Gozzini, A. Lucchesini, Eur. Phys. J. D **28**, 157 (2004)
7. E.B. Alexandrov, M.V. Balabas, D. Budker, D. English, D.F. Kimball, C.H. Li, V.V. Yashchuk, Phys. Rev. A **66**, 042903 (2002)
8. A.M. Bonch-Bruevich, Y.N. Maksimov, S.G. Przhibel'skii, V.V. Khromov, Sov. Phys. JETP **65**, 161 (1987)
9. B.P. Anderson, M.A. Kasevich, Phys. Rev. A **63**, 023404 (2001)
10. A. Burchianti et al., Europhys. Lett. **67**, 983 (2004)
11. M.T. Graf, D.F. Kimball, S.M. Rochester, K. Kerner, C. Wong, D. Budker, E.B. Alexandrov, M.V. Balabas, V.V. Yashchuk, Phys. Rev. A **72**, 023401 (2005)
12. M. Allegrini, P. Bicchi, L. Moi, P. Savino, Opt. Commun. **32**, 396 (1980)
13. X. Zeng, Z. Wu, T. Call, E. Miron, D. Schreiber, W. Happer, Phys. Rev. A **31**, 260 (1985)
14. E. Mariotti, M. Meucci, P. Bicchi, C. Marinelli, L. Moi, Opt. Commun. **134**, 121 (1997)

15. S.N. Atutov et al., Phys. Rev. A **67**, 053401 (2003)
16. S. Du, M.B. Squires, Y. Imai, L. Czaia, R.A. Saravanan, V. Bright, J. Reichel, T.W. Hänsch, D.Z. Anderson, Phys. Rev. A **70**, 053606 (2004)
17. J. Brewer, A. Burchianti, C. Marinelli, E. Mariotti, L. Moi, K. Rubahn, H.G. Rubahn, Appl. Surf. Sci. **228**, 40 (2004)
18. A. Burchianti, Ph.D. thesis, University of Siena (2003)
19. M.A. Bouchiat, J. Brossel, Phys. Rev. **147**, 41 (1966)
20. J.C. Camparo, R.P. Frueholz, B. Jaduszliwer, J. Appl. Phys. **62**, 676 (1987)
21. *Handbook of Physical Quantities*, edited by I.S. Grigoriev, E.Z. Melikhov (CRC Press, Boca Raton, 1997)
22. *Handbook of Atomic, Molecular and Optical Physics*, edited by G.W.F. Drake (Springer, Berlin, 1996)
23. J.H. Xu, A. Gozzini, F. Mango, G. Alzetta, R.A. Bernheim, Phys. Rev. A **54**, 3146 (1996)
24. J. Brewer, V.G. Bordo, M.J. Kasprowicz, H.G. Rubahn, Phys. Rev. A **69**, 062902 (2004)
25. J.C. Camparo, J. Chem. Phys. **86**, 1533 (1987)
26. Z.W. Gortel, H.J. Kreuzer, R. Teshima, Phys. Rev. B **22**, 5655 (1980)
27. A.A. Maradudin, R.F. Wallis, Phys. Rev. B **2**, 4294 (1971)
28. R.F. Wallis, A.A. Maradudin, Phys. Rev. B **3**, 2063 (1970)
29. L.B. Humphreys, Phys. Rev. B **6**, 3886 (1972)
30. J.H. de Boer, *The Dynamical Character of Adsorption* (Clarendon, Oxford, 1968)